Rotating Table with Parallel Kinematic Featuring a Planar Joint

Stefan Bracher*, Luc Baron† and Xiaoyu Wang‡
Ecole Polytechnique de Montréal, C.P. 6079, succ. C.V.
H3C 3A7 Montréal, QC, Canada

Abstract—*In order to develop a rotating table that can be mounted on an existing milling machine and allows operation at high speed, a geometry with two parallel kinematic chains, of which one contains a planar joint, connecting the base to the end-effector, is proposed. The kinematic performances are developed and singularities identified. Computation of the workspace shows that it allows almost all tool vectors that origin from above the table surface and does not include any of the singularities or unstable orientations of the geometry.*

Keywords: parallel kinematic, rotating table, planar joint, rotation-centre above the surface

I. Introduction

In the past few years, several parallel kinematic designs for milling machines [1, 2] have been proposed in order to provide higher operation speed and accuracy. However, most of them are complete machine redesigns what dramatically increases the investment for a new implementation. In order to reduce cost, the proposed mechanism is intended to be mounted on the table of an existing milling machine and working as a tilting table. This combined parallel and serial approach would add a fast orientation changing feature due to the parallel design, while using the existing positioning and spindle mechanisms.

II. The kinematic design

Different possible designs [3-6] have been evaluated based on their robustness and simplicity. The selected mechanism consist of two kinematic chains, the first including two revolute joints and the second including two revolute joints and one planar joint.

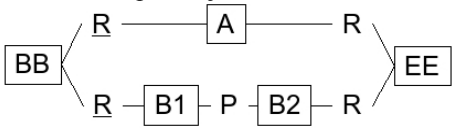

Fig. 1. The kinematic chains of the mechanism

Body A, along the first chain, is connected to the base, namely BB, through an actuated revolute joint (angle θ_1) around the axe $\mathbf{u_1}=\mathbf{x_0}$ and to the end-effector, named EE, through a passive revolute joint around the axe $\mathbf{v_1}=\mathbf{y_t}$. Body B_1, along the second chain is connected to the base BB through an actuated revolute joint (angle θ_2) around the axe $\mathbf{u_2}=\mathbf{y_0}$. Moreover a passive planar joint connects B_1 and B_2, and finally, B_2 and the end-effector EE are linked by a passive revolute joint around the axe $\mathbf{v_2}=\mathbf{z_t}$, where $\mathbf{z_t}$ is the normal vector to the table.

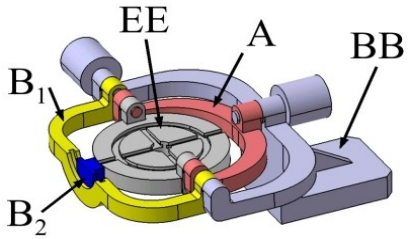

Fig. 2. The kinematic design at $\theta_1=\theta_2=0°$.

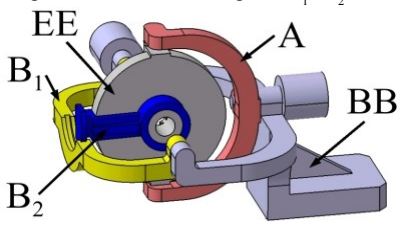

Fig. 3 The kinematic design rotated at $\theta_1=90°, \theta_2=0°$

Thus the orientation of EE is defined by the vectors $\mathbf{v_2}=\mathbf{z_t}$ and $\mathbf{v_1}=\mathbf{y_t}$. For $\theta_1=0°$ and $\theta_2=0°$ the base-coordinate frame {0} and the table-coordinate frame {t} are coincident.

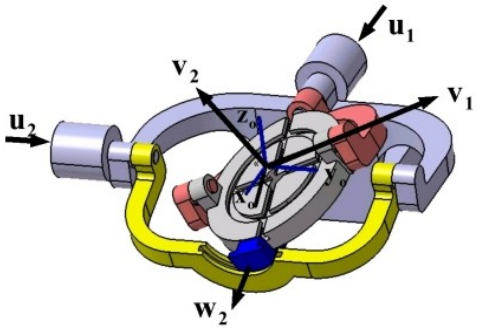

Fig. 4 Base frame {0} and vectors $\mathbf{u_i}$, $\mathbf{v_i}$ and $\mathbf{w_2}$.

The vector perpendicular the plane of the planar joint is called $\mathbf{w_2}$.

$$\mathbf{w_2}=\begin{pmatrix}\cos(\theta_2)\\0\\-\sin(\theta_2)\end{pmatrix}_0 \quad (1)$$

[1]*E-mail: stefan.bracher@polymtl.ca
† E-mail: luc.baron@polymtl.ca
‡ E-mail: xiaoyu.wang@polymtl.ca

All these vectors are unitary and intersect at the rotation-centre, which, as an interesting feature of this design, is situated above the surface of the table.
Unfortunately, the geometry is hyperstatic, making the intersection of the vectors $\mathbf{u_i}$ and $\mathbf{v_i}$ mandatory. This means that a small fabrication error in one of the joints would lock the device movements.
As shown in Fig. 2 and 3, the planar joint could be replaced by a passive revolute joint. The advantages of the planar joint are not obstructed access to the table from the front and a higher position tolerance, as no additional axe that has to go through the rotation-centre is introduced.

III. Inverse Kinematics

As for most parallel robots, the inverse kinematics is straight forward. The unit vector $\mathbf{v_1}$ is defined directly by θ_1 as

$$ {}_0\mathbf{v_1} = \begin{pmatrix} 0 \\ \cos(\theta_1) \\ \sin(\theta_1) \end{pmatrix}_0 \tag{2} $$

and thus θ_1 is given as

$$ \theta_1 = \text{atan2}\left(\frac{{}_0\mathbf{v_1}(3)}{{}_0\mathbf{v_1}(2)}\right) \tag{3} $$

The unit vector $\mathbf{v_2}$ always has to stay parallel to the plane of the planar joint, thus we have

$$ \theta_2 = \text{atan2}\left(\frac{{}_0\mathbf{v_2}(1)}{{}_0\mathbf{v_2}(3)}\right) \tag{4} $$

Contrary to eq. (3), eq. (4) can become undefined as ${}_0\mathbf{v_2}(1)$ and ${}_0\mathbf{v_2}(3)$ can be zero at the same time when $\mathbf{v_2} = \mathbf{y_0}$. In fact, in this position θ_2 can take any angle without affecting the EE orientation.

IV. Direct Kinematics

A. Solution Algorithm

The direct kinematics is more challenging and can not be solved in a single equation but need an algorithm to be computed.
Vector $\mathbf{v_1}$ has already been found in eq. (2). The task is thus to find $\mathbf{v_2}$.

For $\mathbf{v_2}$, we know several constraints:
(a): $\mathbf{v_2} \perp \mathbf{v_1} \rightarrow \mathbf{v_2} \cdot \mathbf{v_1} = 0$
(b): $\mathbf{v_2} \perp \mathbf{w_2} \rightarrow \mathbf{v_2} \cdot \mathbf{w_2} = 0$
(c): $|\mathbf{v_2}| = 1$

Solving this equation system gives:

For ${}_0\mathbf{v_2}(3) \neq 0$:

$$ {}_0\mathbf{v_2} = \begin{pmatrix} \tan(\theta_2)\,{}_0v_2(3) \\ -\tan(\theta_1)\,{}_0v_2(3) \\ {}_0v_2(3) \end{pmatrix}_0 \tag{5a} $$

with

$$ {}_0v_2(3) = \pm\sqrt{\frac{1}{1+\tan(\theta_1)^2+\tan(\theta_2)^2}} \tag{5a.1} $$

However for ${}_0\mathbf{v_2}(3) = 0$, the solution depends on the orientation of $\mathbf{v_1}$ as well as the previous orientation of $\mathbf{v_2}$:

For ${}_0\mathbf{v_2}(3) = 0$ and $\mathbf{v_1} \neq \pm\mathbf{z_0}$ only the solution with $\mathbf{v_2}$ coaxial with $\mathbf{x_0}$ is possible, and hence:

$$ \mathbf{v_2} = \pm\mathbf{x_0} \tag{5b} $$

For ${}_0\mathbf{v_2}(3) = 0$ and $\mathbf{v_1} = \pm\mathbf{z_0}$, it gets even more complicated.

For ${}_0\mathbf{v_2}(3) = 0$, $\mathbf{v_1} = \pm\mathbf{z_0}$ and $\theta_2 \neq \pm 90^\circ$, vector

$$ \mathbf{v_2} = \pm\mathbf{y_0} \tag{5c} $$

solves the system.

For ${}_0\mathbf{v_2}(3) = 0$, $\mathbf{v_1} = \pm\mathbf{z_0}$ and $\theta_2 = \pm 90^\circ$, theoretically, the two solutions $\mathbf{v_2} = \pm\mathbf{y_0}$ and $\mathbf{v_2} = \pm\mathbf{x_0}$ are possible. However, as it is unlikely that the system suddenly jumps 90 degrees, the solution can be found, looking at the past orientation of $\mathbf{v_2}$, as the solution closer to the past orientation will be the most likely.
Thus for ${}_0\mathbf{v_2}(3) = 0$, $\mathbf{v_1} = \pm\mathbf{z_0}$, $\theta_2 = \pm 90^\circ$ and $|\mathbf{v_2}(1)(t-\Delta t)| < |\mathbf{v_2}(2)(t-\Delta t)|$

$$ \mathbf{v_2}(t) = \pm\mathbf{y_0}, \tag{5d} $$

while for ${}_0\mathbf{v_2}(3) = 0$, $\mathbf{v_1} = \pm\mathbf{z_0}$, $\theta_2 = \pm 90^\circ$, $\theta_2 = \pm 90^\circ$ and $|\mathbf{v_2}(1)(t-\Delta t)| > |\mathbf{v_2}(2)(t-\Delta t)|$

$$ \mathbf{v_2}(t) = \pm\mathbf{x_0} \tag{5e} $$

It has to be noted that solution (5e) is unstable, as the end-effector EE can rotate freely around $\mathbf{v_1}$ because $\mathbf{w_2}$ and $\mathbf{v_1}$ are coaxial.

Unfortunately, eqs. (5a-e) always contain two solutions. The angle $\phi = \text{angle}(\mathbf{v_2}(t), \mathbf{v_2}(t-\Delta t))$ has to be computed. As again no jumps can be expected in the real geometry, the solution leading to the smaller angle must be the right one.

With the two obtained vectors, the coordinate frame of EE can be built as

$$ \mathbf{z_t} = \mathbf{v_2},\ \mathbf{y_t} = \mathbf{v_1},\ \mathbf{x_t} = \mathbf{z_t} \times \mathbf{y_t} \tag{6} $$

B. Performance Analysis

To perform an analysis of the direct kinematics, a MATLAB® program has been written that computes the direct kinematics algorithm for all angular combinations.

Because the direct kinematics of a certain angular combination depends on the former orientation, this has been done in two ways:

First way, called "Theta1 first", i.e.,

1. $\Delta\theta_1=\Delta\theta_2=1^o$
2. Initial position: ${}_0\mathbf{v}_2=\begin{pmatrix}0\\1\\0\end{pmatrix}_0$, ${}_0\mathbf{v}_2=\begin{pmatrix}0\\0\\1\end{pmatrix}_0$
3. For $\theta_1=0^o$ to $\theta_1=360^o$ {
   For $\theta_2=0^o$ to $\theta_2=360^o$ {
   Compute direct kinematics
   $\theta_2=\theta_2+\Delta\theta_2$ }
   $\theta_1=\theta_1+\Delta\theta_1$ }

The second way (called "Theta2 first") is the same algorithm, with exchanged roles of θ_1 and θ_2 .

To visualise the result, the direct kinematics solution of $\mathbf{v}_2(1,2,3)$ is displayed in charts as a function of θ_1 and θ_2 .

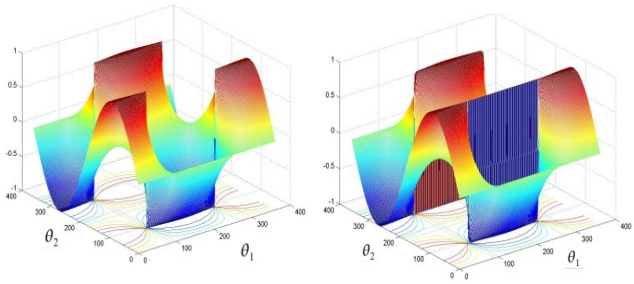

Fig. 5. The values of $\mathbf{v}_2(1)$ if θ_1 is moved first (left) and if θ_2 is moved first (right)

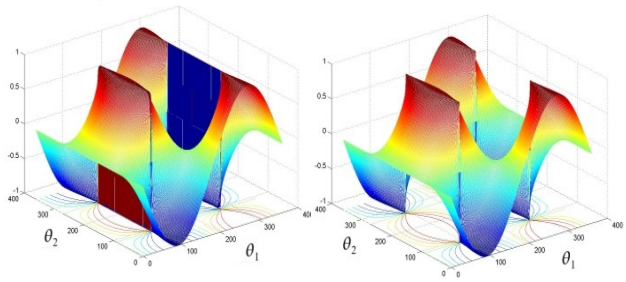

Fig. 6. The values of $\mathbf{v}_2(2)$ if θ_1 is moved first (left) and if θ_2 is moved first (right)

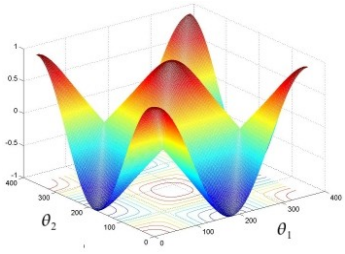

Fig. 7 The values of $\mathbf{v}_2(3)$, independent of the sequence of the movement

It can be observed how drastically the resulting orientation depends on the sequence of the movements as well as the initial orientation.

For example: Starting at $\theta_1=\theta_2=0°$ and turning θ_1 first to +-90° brings the table in a position in which θ_2 has no influence on the orientation. But if θ_1 was not turned exactly to +-90°, θ_2 has a huge influence on the orientation. For θ_1 slightly smaller than 90°, the value of $\mathbf{v}_2(1)$ for $\theta_2=90^o$ is "+1" while for an θ_1 slightly higher than 90° $\mathbf{v}_2(1)=-1$.

Looking at figures 5-7, we see also that the positions where θ_1 and θ_2 are multiples of 90° are special.

For $\theta_1=90^o/270^o, 90^o\le\theta_2\le270^o$ and $90^o\le\theta_1\le270^o, \theta_2=90^o/270^o$ the solutions of the direct kinematics give completely different results for the two operation modes.

V. Jacobian Marix

The orientation of the table is completely constrained by the following three closure equations.

- $\mathbf{v}_2\perp\mathbf{w}_2\Rightarrow\mathbf{v}_2\cdot\mathbf{w}_2=0$ (7)
- $\mathbf{v}_1\perp\mathbf{v}_2\Rightarrow\mathbf{v}_1\cdot\mathbf{v}_2=0$ (8)
- $\mathbf{v}_1\perp\mathbf{u}_1\Rightarrow\mathbf{v}_1\cdot\mathbf{u}_1=0$ (9)

Similar to [7], the Jacobian is based on their time derivations:

$$\frac{d(\mathbf{v}_2\cdot\mathbf{w}_2)}{dt}=\dot{\mathbf{v}}_2\cdot\mathbf{w}_2+\mathbf{v}_2\cdot\dot{\mathbf{w}}_2=0 \quad (10)$$

$$\frac{d(\mathbf{v}_1\cdot\mathbf{v}_2)}{dt}=\dot{\mathbf{v}}_1\cdot\mathbf{v}_2+\mathbf{v}_1\cdot\dot{\mathbf{v}}_2=0 \quad (11)$$

$$\frac{d(\mathbf{v}_1\cdot\mathbf{u}_1)}{dt}=\dot{\mathbf{v}}_1\cdot\mathbf{u}_1=0 \quad (12)$$

In addition we know that

$$\dot{\mathbf{v}}_2=\boldsymbol{\omega}\times\mathbf{v}_2 \quad (13)$$

$$\dot{\mathbf{v}}_1=\dot{\theta}_1\mathbf{u}_1\times\mathbf{v}_1 \quad (14)$$

$$\dot{\mathbf{w}}_2=\dot{\theta}_2\mathbf{u}_2\times\mathbf{w}_2 \quad (15)$$

Inserting eqs. (13) and (15) into eq. (10) gives:

$$\mathbf{u}_2\times\mathbf{w}_2\cdot\mathbf{v}_2\dot{\theta}_2=\mathbf{w}_2\times\mathbf{v}_2\cdot\boldsymbol{\omega} \tag{16}$$

Equations (13) and (14) inserted into (11) produce:

$$\mathbf{u}_1\times\mathbf{v}_1\cdot\mathbf{v}_2\dot{\theta}_1=\mathbf{v}_1\times\mathbf{v}_2\cdot\boldsymbol{\omega} \tag{17}$$

To solve eq. (12) another relation of $\dot{\mathbf{v}}_1$ is used, i.e.:

$$\dot{\mathbf{v}}_1=\boldsymbol{\omega}\times\mathbf{v}_1 \tag{18}$$

Finally eq. (18) inserted into eq. (12) leads to

$$\mathbf{u}_1\times\mathbf{v}_1\cdot\boldsymbol{\omega}=0 \tag{19}$$

Equation (19) suggests a new rule:

$$\boldsymbol{\omega}\perp(\mathbf{u}_1\times\mathbf{v}_1)$$

thus $\boldsymbol{\omega}=\begin{bmatrix}\omega(1)\\ \omega(2)\\ \tan(\theta_1)\omega(2)\end{bmatrix}$ (20)

which, looking at the geometry, makes sense as body A prevents any rotation around $(\mathbf{u}_1\times\mathbf{v}_1)$.

With the eqs. (16), (17) and (20), the matrices **A** and **B**, that connect the rotation of the articulated joints to the rotation of the table, become:

$$\mathbf{A}\begin{bmatrix}\dot{\theta}_1\\ \dot{\theta}_2\end{bmatrix}=\mathbf{B}\,\boldsymbol{\omega}$$

$$\begin{bmatrix}0 & \mathbf{u}_2\times\mathbf{w}_2\cdot\mathbf{v}_2\\ \mathbf{u}_1\times\mathbf{v}_1\cdot\mathbf{v}_2 & 0\\ 0 & 0\end{bmatrix}\dot{\boldsymbol{\theta}}=\begin{bmatrix}(\mathbf{w}_2\times\mathbf{v}_2)^{\mathrm{T}}\\ (\mathbf{v}_1\times\mathbf{v}_2)^{\mathrm{T}}\\ (\mathbf{u}_1\times\mathbf{v}_1)^{\mathrm{T}}\end{bmatrix}\boldsymbol{\omega} \tag{21}$$

For the application however, the combined Jacobian's

$$\mathbf{J}_{\theta\to\omega}\dot{\boldsymbol{\theta}}=\boldsymbol{\omega} \tag{22}$$

and

$$\dot{\boldsymbol{\theta}}=\mathbf{J}_{\omega\to\theta}\boldsymbol{\omega} \tag{23}$$

are more useful.

Looking at eq. (21) it is clear that

$$\mathbf{J}_{\theta\to\omega}=\mathbf{B}^{-1}\mathbf{A} \tag{24}$$

and

$$\mathbf{J}_{\omega\to\theta}=\mathbf{A}^{-1}\mathbf{B} \tag{25}$$

$\mathbf{J}_{\theta\to\omega}$ can be computed without problems for most cases. A general $\mathbf{J}_{\omega\to\theta}$ on the other hand is not existing as **A**, being a rectangular matrix, is not invertible. There can not be a $\mathbf{J}_{\omega\to\theta}$ that solves eq. (23) for any $\boldsymbol{\omega}$, because, as eq. (20) implies, not all $\boldsymbol{\omega}$ are possible.

But going with by eq. (20) admitted $\boldsymbol{\omega}$, $\boldsymbol{\omega}^{\mathrm{x}}$, in eq. (21), we can eliminate the last line:

$$\mathbf{A}^{\mathrm{x}}\dot{\boldsymbol{\theta}}=\mathbf{B}^{\mathrm{x}}\boldsymbol{\omega}^{\mathrm{x}}$$

$$\begin{bmatrix}0 & \mathbf{u}_2\times\mathbf{w}_2\cdot\mathbf{v}_2\\ \mathbf{u}_1\times\mathbf{v}_1\cdot\mathbf{v}_2 & 0\end{bmatrix}\dot{\boldsymbol{\theta}}=\begin{bmatrix}(\mathbf{w}_2\times\mathbf{v}_2)^{\mathrm{T}}\\ (\mathbf{v}_1\times\mathbf{v}_2)^{\mathrm{T}}\end{bmatrix}\cdot\vec{\omega}^{\mathrm{x}} \tag{26}$$

And $\mathbf{J}^{\mathrm{x}}_{\omega\to\theta}=\mathbf{A}^{\mathrm{x}-1}\mathbf{B}^{\mathrm{x}}$ (27)

can be found, but is only valid for previously checked $\boldsymbol{\omega}^{\mathrm{x}}$.

VI. Singularities

Special interest has to be put in the orientations that make either **A** or **B** lose another rank.

For **A,** this is the case when either:

$$-\ \mathbf{v}_2=\pm\mathbf{u}_2\rightarrow\mathbf{u}_2\times\mathbf{w}_2\cdot\mathbf{v}_2=0 \tag{28}$$

$$-\ \mathbf{v}_2=\pm\mathbf{u}_1\rightarrow\mathbf{u}_1\times\mathbf{v}_1\cdot\mathbf{v}_2=0 \tag{29}$$

and **B** when either:

$$-\ \mathbf{v}_1=\pm\mathbf{w}_2\rightarrow\mathbf{w}_2\times\mathbf{v}_2=\pm\mathbf{v}_1\times\mathbf{v}_2 \tag{30}$$

$$-\ \mathbf{v}_2=\pm\mathbf{u}_1\rightarrow\mathbf{v}_1\times\mathbf{v}_2=\pm\mathbf{u}_1\times\mathbf{v}_1 \tag{31}$$

$$-\ (\mathbf{v}_2=\pm\mathbf{u}_1)\wedge(\mathbf{v}_1=\pm\mathbf{w}_2)\rightarrow\mathbf{w}_2\times\mathbf{v}_2=\pm\mathbf{u}_1\times\mathbf{v}_1 \tag{32}$$

In the cases of eq. (28) and (29) **A** and $\mathbf{A}^{\mathrm{x}}$ are not invertible and $\mathbf{J}^{\mathrm{x}}_{\omega\to\theta}$ can not be computed directly, as in addition to eq. (20), some other criteria have to be met for admissible $\boldsymbol{\omega}$.

$\mathbf{J}^{\mathrm{x}}_{\theta\to\omega}$, on the other hand, is not computable for the cases of eqs. (30-32).

But even when the inverse of **A** or **B** is not existing, there still is a Jacobian. To obtain it, the system has to be solved analytically. Let's see what happens exactly in these cases:

$-\ \mathbf{v}_2=\pm\mathbf{u}_2$:

Geometrical constraint: $\mathbf{v}_1=\pm\mathbf{z}_0$ (33)

Admissible $\boldsymbol{\omega}^{\mathrm{xx}}$: $\boldsymbol{\omega}^{\mathrm{xx}}=\omega\,\mathbf{w}_2$ (34)

Jacobian's that solve the equation system:

$$\mathbf{J}^{\mathrm{xx}}_{\omega\to\theta}=\begin{bmatrix}1 & 0 & 0\\ 0 & 0 & 0\end{bmatrix},\quad \mathbf{J}_{\theta\to\omega}=\begin{bmatrix}1 & 0\\ 0 & 0\\ \dfrac{\mathbf{w}_2\cdot\mathbf{z}_0}{\mathbf{u}_1\cdot\mathbf{w}_2} & 0\end{bmatrix} \tag{35}$$

$^{\mathrm{xx}}$ for admissible $\boldsymbol{\omega}^{\mathrm{xx}}$

$\rightarrow$ Singularity in $\mathbf{J}_{\theta\to\omega}$ and Instability:

$$\mathbf{w}_2=\pm\mathrm{z}_{0,}\ \mathbf{v}_2=\pm\mathbf{u}_{2,}\ \mathbf{v}_1=\pm\mathbf{z}_0 \tag{36}$$

$-\ (\mathbf{v}_2=\pm\mathbf{u}_1)\wedge(\mathbf{v}_1\neq\pm\mathbf{w}_2)$:

Geometrical constraint: $\mathbf{w}_2=\pm\mathbf{z}_0$ (37)

Admissible $\boldsymbol{\omega}^{\mathrm{xx}}$: $\boldsymbol{\omega}^{\mathrm{xx}}\perp(\mathbf{u}_1\times\mathbf{v}_1)$ (38)

Jacobian's that solve the equation system:

$$\mathbf{J}^{xx}_{\omega\to\theta}=\begin{bmatrix}1&0&0\\0&1&0\end{bmatrix},\ \mathbf{J}_{\theta\to\omega}=\begin{bmatrix}1&0\\0&1\\0&\tan(\theta_1)\end{bmatrix} \quad (39)$$

^{xx} for admissible $\boldsymbol{\omega}^{xx}$

- $(\mathbf{v}_2=\pm\mathbf{u}_1)\wedge(\mathbf{v}_1=\pm\mathbf{w}_2)$:

Geometrical constraint: $\mathbf{w}_2=\pm\mathbf{z}_0$ (40)

Admissible $\boldsymbol{\omega}^{xx}$: $\boldsymbol{\omega}^{xx}\perp(\mathbf{u}_1\times\mathbf{v}_1)=\boldsymbol{\omega}^{xx}\perp\mathbf{y}_0$ (41)

Jacobian's that solve the equation system:

$$\mathbf{J}^{xx}_{\omega\to\theta}=\begin{bmatrix}1&0&0\\0&1&0\end{bmatrix},\ \mathbf{J}_{\theta\to\omega}=\begin{bmatrix}1&0\\0&1\\0&\pm\infty\end{bmatrix} \quad (42)$$

^{xx} for admissible $\boldsymbol{\omega}^{xx}$

→ Singularity in $\mathbf{J}_{\theta\to\omega}$ and Instability:

$\mathbf{v}_1=\pm z_0,\ \mathbf{v}_2=\pm\mathbf{u}_1$ (43)

- $(\mathbf{v}_1=\pm\mathbf{w}_2)\wedge(\mathbf{v}_2\neq\pm\mathbf{u}_1)$:

Geometrical constraints: $\mathbf{w}_2=\pm\mathbf{z}_0$, $\mathbf{v}_2=\pm\mathbf{u}_2$ (44)

→ see eqs. (33) to (36).

VII. Workspace

After having determined the singularities, it is also important to take account of the geometrical constraints, such as collisions and obstructions, to finally obtain the available workspace.

A. Workspace computation

An algorithm has been written to compute the workspace in form of a sphere, where every surface point corresponds to a tool-axis orientation in the end-effector-, the tool table frame.

In a first step, the possible end-effector positions in which the demanded tool-axis is coincident with $\mathbf{z}_0$, so it matches the spindle, are produced. According to the two modes of operation, this is done either by changing first θ_1 and then θ_2, or the other way around.

For the obtained end-effector orientations, the necessary angles are obtained with the inverse kinematics and then used to calculate $\mathbf{J}_{\theta\to\omega}$. In the next step, $\mathbf{J}_{\theta\to\omega}$ is analysed and assigned a value depending of it's properties. A verification is done, if the demanded orientation causes a violation of the maximal possible angles or if there is obstruction by a member that prevents operation of the tool at the position. If so, the corresponding surface point on the sphere is removed, thus showing only possible orientations in the figures. Finally it is checked if the table causes an obstruction. If so, the corresponding point is "shaded". This case of obstruction is treated differently than the one by a member of the kinematic chains, because it occurs whenever a table is used to mount a piece and thus is not related to the geometry itself.

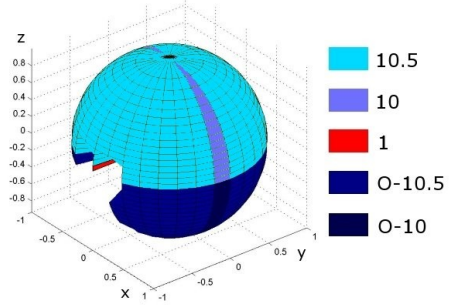

Fig.8. Workspace for turning first around $\mathbf{u}_1$ and then around $\mathbf{v}_1$ (changing θ_1 before θ_2)

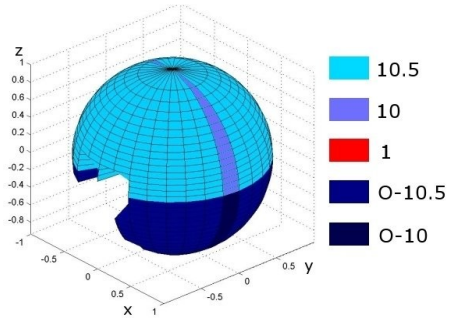

Fig.9 Workspace for turning first around $\mathbf{v}_1$ and then around $\mathbf{u}_1$ (changing θ_2 before θ_1)

Value	*Meaning*
1	$\mathbf{J}_{\theta\to\omega}=\begin{bmatrix}a&0\\0&0\\0&0\end{bmatrix}$ Or $\mathbf{J}_{\theta\to\omega}=\begin{bmatrix}0&a\\0&0\\0&0\end{bmatrix}$
10	$\mathbf{J}_{\theta\to\omega}=\begin{bmatrix}\mathbf{a}'\\\mathbf{b}'\\\mathbf{0}\end{bmatrix}$
10.5	$\mathbf{J}_{\theta\to\omega}=\begin{bmatrix}\mathbf{a}'\\\mathbf{b}'\\\mathbf{c}'\end{bmatrix}$
O-10	Like 10, but access obstructed by the table
O-10.5	Like 10.5, but access obstructed by the table

Fig.13. The assigned Jacobian values occurring in the workspace

The geometry parameters used for the computation of figures 8 and 9:

- $-100^o<\theta_1<100^o$: For values outside this range B_2 would not be in contact with B_1 thus destroy the planar joint.
- $-160^o<\theta_2<100^o$: $\theta_2<-160^o$ * would cause a collision between B_1 and A , $\theta_2>100^o$ * a collision between B_1 and the support.
- Collision range =20°*: the maximal possible

approximation to ($\mathbf{v_2}=\pm\mathbf{u_1}$, $\mathbf{v_1}=\pm\mathbf{z_0}$) without causing a collision between a A and B_1 or B_2 .
- Rotation-centre on the table surface.

* exact values depending on geometry parameters such as thickness of A , B_1 , B_2 and the outer diameter of planar joint.

B. Observations

The available, non obstructed workspace (values 10.5, 10 and 1 in figures 8 and 9) is basically a half-sphere without areas around y=+-1 . The areas around y=+-1 are lost because of collisions between A and B_1 when approaching ($\mathbf{v_2}=\pm\mathbf{u_1}$, $\mathbf{v_1}=\pm\mathbf{z_0}$) and obstruction by A for θ_1 close to $\pm 100^{o}$. Thus, placing the the rotation-centre higher above the table surface decreases the, by the table obstructed part of the workspace, but increases the lost areas around y=+-1. Making A , B_1 and B_2 as thin as possible while setting the inner radius of B_1 bigger that the diagonal size of A reduces the lost area independent of the rotation-centre position.

The good news however is that none of the singularities or unstable points are included in the workspace. This, because the critical end-effector orientations described under point VI either are not needed or can not be exploited due to obstruction or collision.

VIII. Conclusion

The parallel geometry studied showed to be without singularities when operated within the limits given by the workspace, what allows almost all tool vectors that origin above the working table. The chain combination (see fig. 1) is hyperstatic what renders manufacturing a difficult task. A fabrication error resistant geometry might be obtained by adding a prismatic joint in B_2 between the planar and the revolute joint, so that $\mathbf{u_2}$ does not need to intersect exactly with the rotation-centre.

The main advantage of the introduction of the planar joint is, that the rotation centre can be placed above the table surface without causing obstruction for all the access vectors in, and close to the table plane. Those of these vectors that are still not realisable are repressed by the revolute joint along $\mathbf{v_1}$. The type of planar joint used could be transformed into a revolute joint by making the ground surface of the chamfer as well operational. It would be interesting to study if utilisation of such a modified revolute joint along $\mathbf{v_1}$ would be able to remove the obstructions of the classical joint while not adding too many other constraints.

For the implementation of the rotating table, it is necessary to find a way to protect the operational surfaces of the planar joint against chips that could cause a blockage or reduce the accuracy.

An important part of the work that has yet to be done is the development of a suitable controller. It has to combine the control of the positioning part, realised by the serial axis of the existing machine on which the rotating table is mounted, with the control for the parallel, orientation part. A good approach might be to take advantage of already implemented controllers for the serial part in order to limit the number of controller variations needed for different machine types.

Another challenge for the controller will be to switch adequately between the different operation modes (θ_1 first and θ_2 first) and to avoid the postures causing collisions and obstructions.

References

[1] W.J. Blümlein. The Hexapod. *Machine+Werkzeug 10/99,* September 1999.

[2] M. Hebsacker. Entwurf und Bewertung Paralleler Werkzeugmaschinen - das Hexaglide. *ETH Zürich*, 2000.

[3] M. Sabsaby Synthèse d'un manipulateur parallèle sphérique à trois degrés de liberté. *Université de Montréal,* January 2002.

[4] S. Brunet. Synthèse géométrique d'un manipulateur parallèle sphérique à trois degrés de liberté. *Université de Montréal,* December 2003.

[5] S. Mamdouh. Solution du problème géométrique directe des manipulateurs de topologie STAR. *Université de Montréal,* 2004.

[6] J-P..Merlet. Manipulateurs pour orientation/ Orientation robots. *http://www-sop.inria.fr/coprin/equipe/merlet/Archi/node8.html*

[7] C. Gosselin, J. Angeles. The optimum kinematic design of a spherical three-degree of freedom parallel Manipulator. *ASME Journal of Mechanisms, Transmissions and Automation in Design,* Vol.111, June 1989.